GLOBAL OPTIMIZATION OF TWO-DIMENSIONAL HIGH LIFT AERODYNAMIC SYSTEM

Hospodář P.*, Szöllös A.*, Vrchota P.*
***Aeronautical Research and Test Establishment, Prague, Czech Republic**
hospodar@vzlu.cz; szollos@vzlu.cz; vrchota@vzlu.cz

Keywords: *DOE, RSM, microGA, CFD*

Abstract

A quasi-global optimization procedure is presented in this paper. It is used for the optimal placement of multi-element high lift system in landing configuration. A goal of the optimization is to maximize lift. Design of Experiment and Response Surface Method is used for preliminary mapping of design area and as a determination of an initial vector for Evolutionary optimization. Micro Genetic Algorithm with very small population is used to find the optimal setting of the high-lift system.

1 Introduction

Computational Fluid Dynamic (CFD) plays an important role in the aerodynamic design of the airplane. The High-Lift System (HLS) belongs to one of the most difficult part of the aerodynamic design. The principal challenge in the design of HLS is the complex nature of the flow. The dominant flow features include regions od separated flow, confluent boundary layers and regions with supersonic flow [1], [2]. Although the CFD has been highly developed and improved, these flow features still strongly impose additional requirements on the accuracy of the CFD.

The primary goal of the HLS is to increase the payload capacity and reduce the take-off and landing distances. This is achieved by increasing the lift coefficient at given angle of attack and increasing the maximum lift coefficient, as well. The optimized configuration can significantly improve the aerodynamic performances, as well as reduce the mechanical complexity and provide weight savings. The top of complexity of HLS was achieved at the end of seventies (B-747, e.g.), meanwhile the current HLS become simpler then the previous one (A-380) [3]and has to be highly optimized to achieve or to improve all the requirements on the aerodynamic performances.

The main motivation of this study is twofold. On the one hand we would like to improve the landing performance of an existing high-lift system using combination of Surrogate Based Model and the Evolutionary Algorithms. On the other hand we would like to setup a numerical design optimization procedure that can be useful to the aerodynamicist in the rapid design and development of HLS configuration regarding the influence of various design parameters (gap, overlap, slat and flap deflection angles, etc.) on the system's performance.

2 Baseline Configuration and Flow solver

2.1 Baseline Configuration

A three-element airfoil with a slat and a single slotted flap is used for this case (see Fig. 1). The chord of the flap is 20% of the chord of the airfoil. The landing configuration was selected for this study (the range limitation of the design variables of the slat and flap).

The wind tunnel test of this baseline configuration for different position of the slat and flap was performed at VZLU, Aeronautical Research and Test Establishment, [4]. The model was hinged on a balance to measure lift, drag and pitching moment. The surface pressure distributions were measured using pressure block built into the model

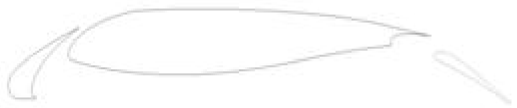

Fig. 1 Baseline configuration

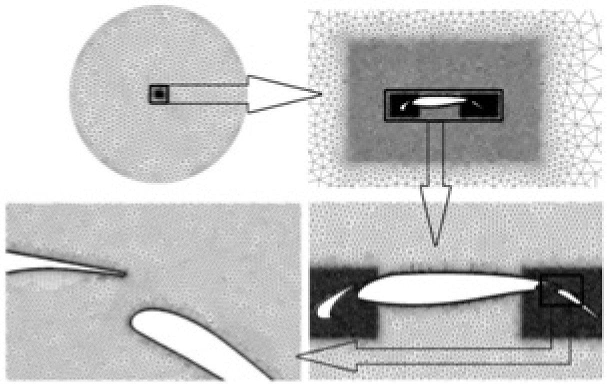

Fig. 2 An overview of 2D mesh; from domain up to boundary layer

2.2 Mesh Generation and Flow Solver

A hybrid unstructured grid with prismatic layers, defining the airfoil geometry and simulating the boundary layer, was used due to the simplicity of creating such grids on complex geometries. The meshes are automatically generated for each set of design parameters using a commercial software package ICEM CFD. ICEM CFD creates an Euler mesh that is used as an input to meshing program TRITET [5], that generates a suitable mesh for Reynolds-Averages Navier-Stokes (RANS) computations. The near-wall grid spacing normal to the wall was set to obtain y+ ≈ 1 based on turbulent flap plate boundary-layer thickness estimate at the Reynolds number in question, Re = 1.65x10^6.

The mesh was refined in close proximity of the slats and the flap to assure that the new slat or flap position in the design space will be inside the fine mesh region and the wakes will be captured well (see Fig. 2).

The RANS equations are solved in EDGE [6], FOI's in-house computational fluid dynamic (CFD) program package. It is a finite volume Navier-Stokes solver for unstructured meshes. It employs local time-stepping, local low-speed preconditioning, multigrid and dual-time-stepping for steady state and time-dependent problems. The data structure of the code is edge-based so that the code is constructed as cell-vertex. It can be run in parallel on a number of processors to efficiently solve large flow cases. It is equipped with a number turbulence model based both on the eddy-viscosity and an explicit algebraic Reynolds stress model (EARSM) assumption. Hellsten k-ω explicit algebraic Reynolds-stress turbulence model was used for this study [7].

2.2.1 Flow condition

The chord-based Reynolds number of $Re = 1.65 \cdot 10^6$ and freestream Mach number of M = 0.18 were used. All cases were calculated in the range of the angle of attack (AoA) around stall conditions (AoA from 15 up to 27 deg). This range was selected with respect to the aim of this task to maximize the C_L and to assure that the stall angle will be achieved. All cases considered in this study were assumed to be fully turbulent, and therefore, the laminar-turbulent trip terms are not used.

3 Methodology

3.1 Design of experiment and Response Surface Method

3.1.1 Design of Experiment

Design of experiment (DOE), is a statistical method that appropriately places design points to determine the functional values in the searching space. Classical DOE methods have been used successfully for several decades. The DOE term covers the system of methods that are used to build a relation between several input design parameters and one or several responses [8], [9].

For the modeling part of the DOE a large number of fractional factorial designs have been developed, such as Box-Behnken design, Latin square design, Box-Wilson (Central Composite) design (CCD). One of the most popular design is the CCD. A different type of design are Taguchi design, Nested design, etc.

The design chosen for this study was central composite design (CCD) for six design factors. It was full factorial 2-level portion design with 77 runs. It consists of the factorial portion of the design, centerpoint portion and axial portion. Design space was chosen on normalized interval for all coded variables [-1;1].

3.1.2 Response Surface Method

The advantages of RSM are that it gives overview of cost function behavior at complete design space, allows simple addition of supplemental requirements to cost function and requires relatively small number of design points for direct cost function evaluation (when DOE theory is used for their choice). As a result of last sentence one of the most important advantages obtained by using RSM in optimization is a significant reduction in the computational cost. Amount of computational effort needed is somewhere between sensitivity based optimization (Adjoint method) and evolutionary optimization (GA). The cost function can be defined after evaluation of the design points. A different cost functions can be applied meanwhile the number of design points remains the same. This allows the user to perform global optimization and reliability-based optimization, which are otherwise prohibitively computationally expensive. In many RSM applications, either linear or quadratic polynomials are assumed to accurately model the observed response values.

The most frequently used response surface model is a second-order containing primary effects, their interaction, and quadratic effects for arbitrary k input factors x_i and output variable y, see Eq. 1.

$$y = \beta_0 + \sum_{i}^{k} \beta_i x_i + \sum_{i}^{k} \beta_{ii} x_i^2 + \sum_{i<j}^{k} \beta_{ij} x_i x_j \qquad (1)$$

Where output variable y represents cost functions, x_i are design parameters and β_i are the unknown polynomial coefficients.

Although the second-order model is one of the most widely used it turned out that it is not sufficiently accurate in this study. It was the main reason why the semi-cubic model was used (see Eq.3) instead of quadratic model.

$$y = \beta_0 + \sum_{i}^{k} \beta_i x_i + \sum_{i}^{k} \beta_{ii} x_i^2 + \sum_{i}^{k} \beta_{iii} x_i^3 \qquad (2)$$

Comparison between the quadratic and semi-cubic RSM is depicted Fig. 3. From residuals and histogram of residuals is it possible to see smaller estimation error for semi-cubic RSM. In the bottom part of the Fig. 3 is shown that the values of normal probability are distributed along straight line quite well. This is the check that the normal distribution adequately describes the data.

3.1.3 Design Variables

Totally six design parameters defining both the position and deflection of the slat and flap were chosen. The detail of the design spaces of the slat and flap are depicted in Fig. 4 and 5. It is possible to see the stowed and deflected positions of the high-lift devices and the design space of the slat and flap, as well (rectangles).

The coordinate systems of the slat and flap were rotated in order to better placing of the design space around the predicted optimal position (see Fig. 4 and 5). The design variables and their limits in natural form are in Tab. 1. The values in the table are relative to the initial position of the high-lift system.

3.1.4 Cost Functions

Selection of the appropriate cost function is a key factor for optimization. Any optimization algorithm will have its advantages and drawbacks, but

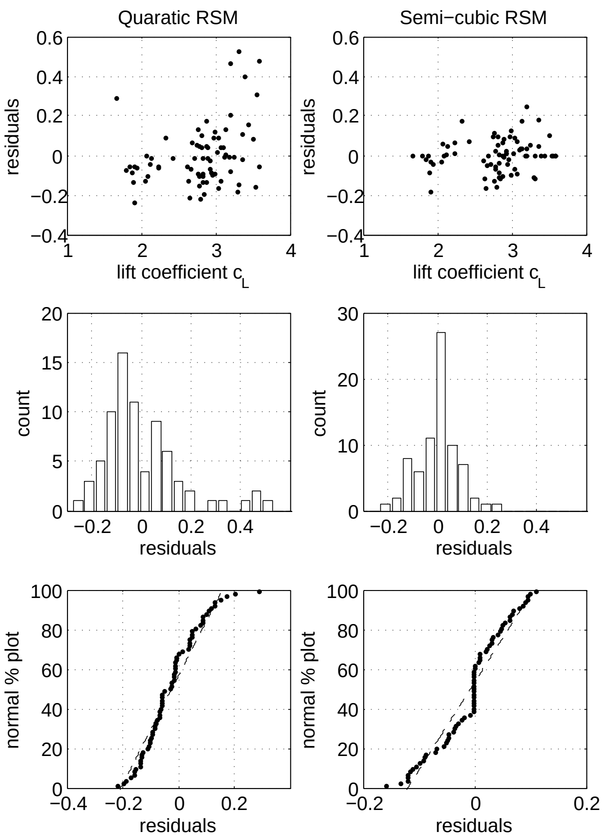

Fig. 3 RSM residual, histogram of residual and normal probability plots

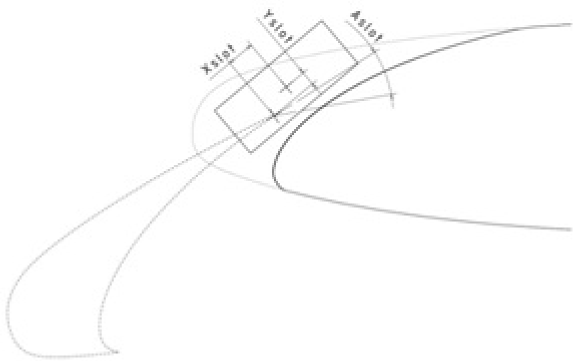

Fig. 4 Detail of the slat design space

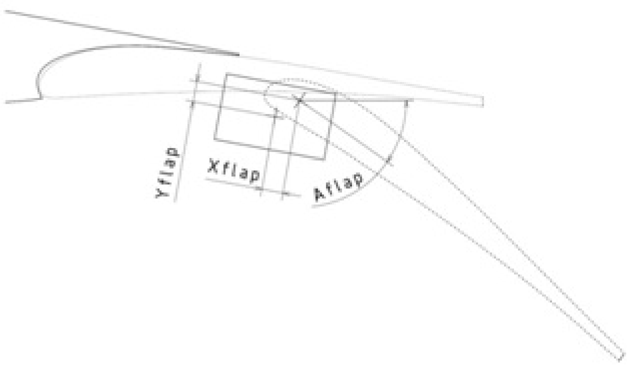

Fig. 5 Detail of flap design space

Table 1 Limits of design variables

Design variable	upper limit	lower limit
Slat x position [mm]	-25	25
Slat y position [mm]	3.5	23.5
Slat deflection [deg]	-20	-25
Flap x position [mm]	-12	18
Flap y position [mm]	-18	0
Flap deflection [deg]	-5	5

when the target of optimization is misleading, the result will be simply useless.

Two cases were consider to optimized. The first task was the lift maximization. The second one was the maximization of the 3rd value of C_L. It means that the values of the lift coefficient were firstly ranked from the largest to smallest and after that the 3rd largest value was used as the cost function. This second procedure is similar to the lift maximization at a fixed angle of attack. It is more time consuming, nevertheless gives better overview about the shape of the lift curve.

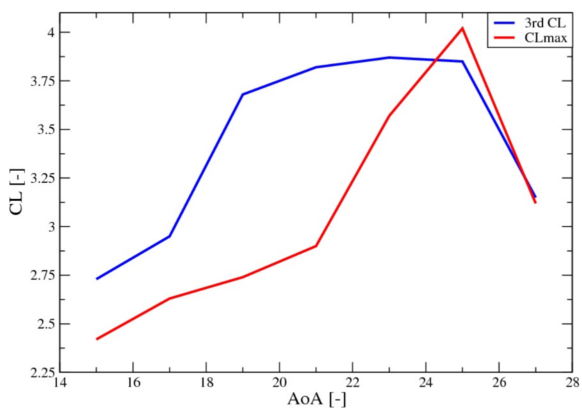

Fig. 6 Effect of the cost function on lift curve

The first was motivated by increasing of the maximum lift coefficient and the second one was considered in order to avoid the undesirable behavior of the lift coefficient shown in Fig. 6 (abrupt increase in slope just prior to reaching maximum lift, which is due to reattachment of the flow on the upper part of the flap, red curve).

3.2 Multi-Objective Micro-Genetic Algorithm with Range Adaptation - μARMOGA

The population evaluation is often time-consuming therefore it is necessary to reduce their number as far as possible. In the extreme case, one can arrive to the so called micro-genetic algorithm using as much as four or five individuals. On the other hand, it is necessary to search as big part of the design space as possible, which is enabled by the range adaptation. This concept was introduced by M. Arakawa and A. Hagiwara [11]. A. Oyama [12] used it in real coding.

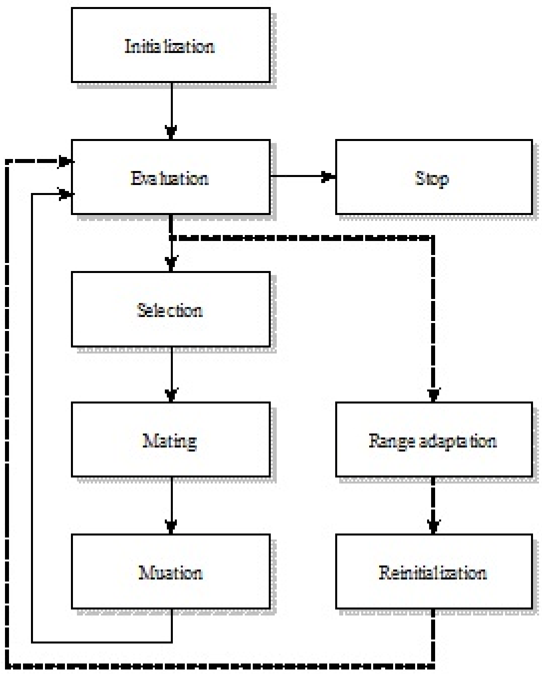

Fig. 7 Flowchart of a multi-objective genetic algorithm with range adaptation and reinitialization

In an attempt to join the advantages of both concepts, we proposed a multi-objective micro-genetic algorithm with range adaptation – μARMOGA. See its flowchart on Fig. 7. Initial population is created by the Mersenne-Twister-random number generator coupled with Latin hypercube sampling and is evaluated for Pareto-dominance. Then individuals for mating are selected via tournament selection. The crossover scheme used is the conventional N-point rule, however in real domain. Eventually, a selected design candidate is mutated by the uniform mutation scheme. Reinitialization takes place once in N-generation together with range-adaptation. More details can be found in [13] and [14].

4 Results

Because of the narrow range of the practical usage of the lift curve for the maximization of the C_L (red lift curve in Fig. 6), only the results of the second cost function (3rd C_L) are presented in this section.

4.1 Validation

A nonoptimal position of the high-lift systems was selected from [4] to verify the possibilities and abilities of the flow solver and also the optimization method to capture the flow separation and to find optima from the worse initial case. This case was characterized by massive flow separation on the flap. Figure 8 shows surface pressure distributions for the experimental and computational results which correspond to the angle of attack 12 deg.

The agreement between experimental and computational distribution is very encouraging. Integral force coefficients also agree quite well. The computation slightly underestimates the size of separated area on the flap.

The calculations were stopped after 4000 iterations. It was proved that this number of iterations is sufficient, for all range of angle of attack, and the changes of residuals were negligible and stable oscillations of aerodynamic forces was achieved, even if the flow separation was occurred (see Fig. 9).

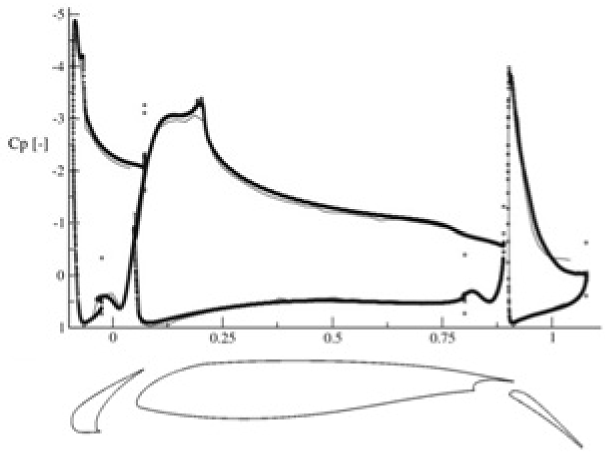

Fig. 8 Comparison of the surface pressure distribution from CFD and experiment

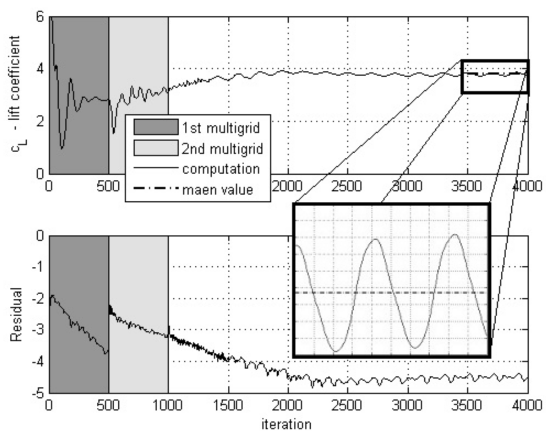

Fig. 9 Convergence history of C_L and residual for multi-element airfoil with highlighted 1^{st} and 2^{nd} multigrid and determination of mean value for resulting C_L

4.2 DoE Results

Optimization of the HLS was carried out using DOE. In the first stage all design parameters were screened to find out if some parameters are unimportant and can be ruled out. The second one was so called modeling stage, the Response Surface was constructed and used to find locus of optimal configuration.

Figure 10 shows Pareto graphs of main effect for the lift coefficient. As can be seen to most significant parameters are those corresponding to the horizontal position and deflection of the slat. On the flap side, the significant parameter is horizontal position of the flap towards the main airfoil. The main effects are slightly distorted by the rotation of the design space and the local coordinate systems of the slat and flap. From the global coordinate system point of view, the particular change in the x and y direction were not independent and influenced each other.

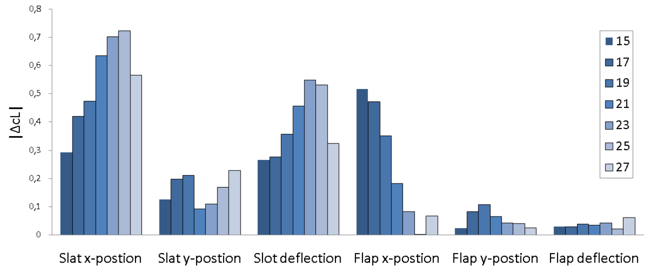

Fig. 10 Pareto graph of high-lift system, main effects of factors

Although the Pareto graphs showed that the deflection and the vertical position of the flap towards the main airfoil did not have significant effect on the lift coefficient, it was decided to optimize all six design parameters by means of μARMOGA. The reason for this decision was the character of the flowfield and selected cost functions (optima of the cost functions located close to the stall angle). The slat prevail the effect of the flap in the range of the of the optima of the cost functions (flow on the flap is usually attached for high AoA, but slat operates in close to the critical conditions). As soon as AoA exceeded certain value, the flow on the slat was separated and the C_L was significantly decreased and the flap was not able to improve it even though the flap was without separation.

4.3 RSM Results

As it was mentioned in the section 3.1.2, one of the main advantage of this procedure is that there is no need to recalculate the design points when the cost function is changed.

The lift curve for the locus optima of the design parameters from response surface is depicted in Fig. 11. The circles symbolize the separate or attached flow on the slat and flap. The variance of the C_L is depicted as well.

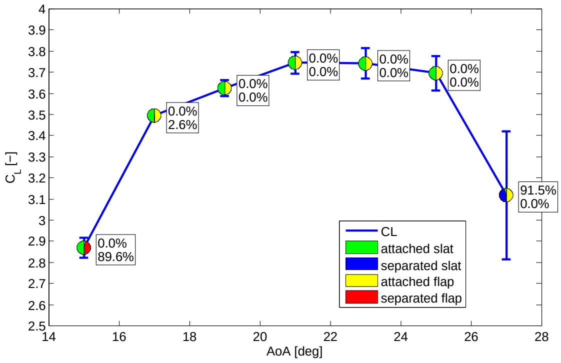

Fig. 11 RSM - lift curve

The flowfield with streamlines is depicted in Fig. 12. The flow separation was completely removed and the C_L was increased approximately about 20% in comparison with the baseline configuration. This optima vector design was used as initial for optimization by μARMOGA.

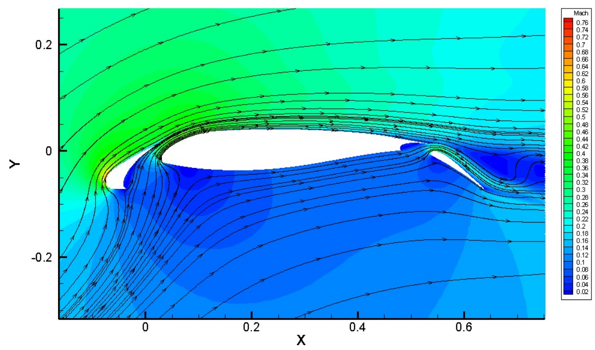

Fig. 12 Flowfield from RSM design

4.4 μARMOGA Results

The evolution of the cost function is depicted in Fig. 13. It is possible to see that the cost function reached the optima after 16 iterations and after that is more or less stagnant. The variance among the particular individuals within the population after 16 iterations is also very small.

The evolution of the particular design parameters is depicted in Fig. 14. The faster convergence was observed for slat deflection and vertical position of the flap. The rest of design parameters converged slowly. This is the reason for the

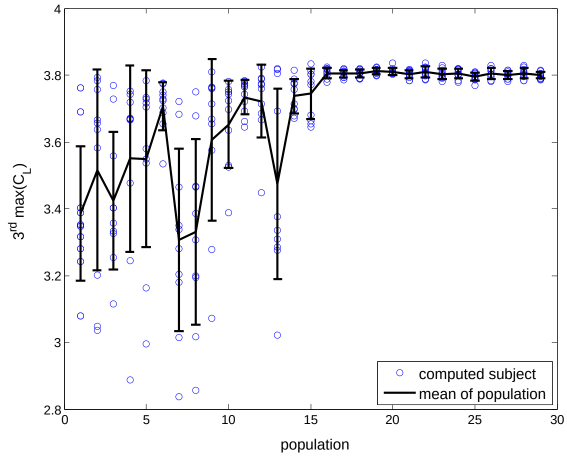

Fig. 13 Cost function evolution

small oscillation of the mean value of cost function after 16 iteration.

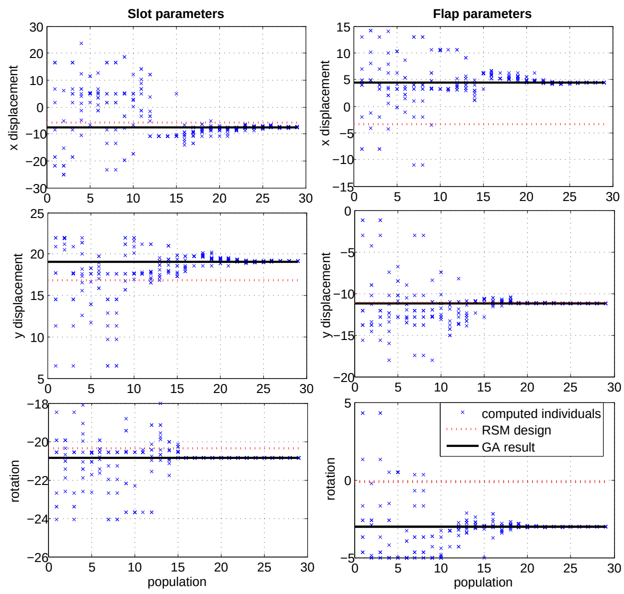

Fig. 14 Parameters evolution

The final lift curve is depicted in Fig. 15. The C_L was increased about 4% in comparison with the initial design from RSM. The exploitable range of AoA was slightly reduced.

The optimized position together with the RSM initial position and the position corresponded to the both cost functions for the slat and flap are depicted in Fig. 16 and Fig. 17, respectively.

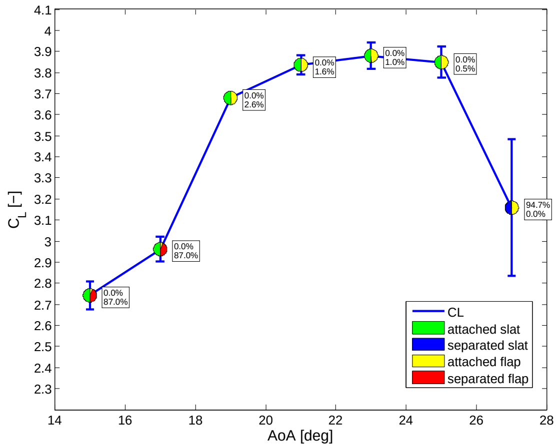

Fig. 15 Lift curve - optimized position

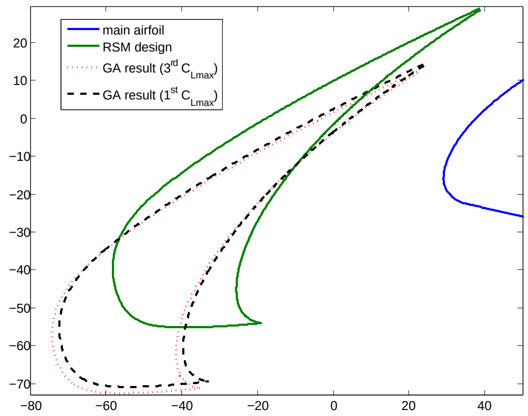

Fig. 16 Slat - optimized positions

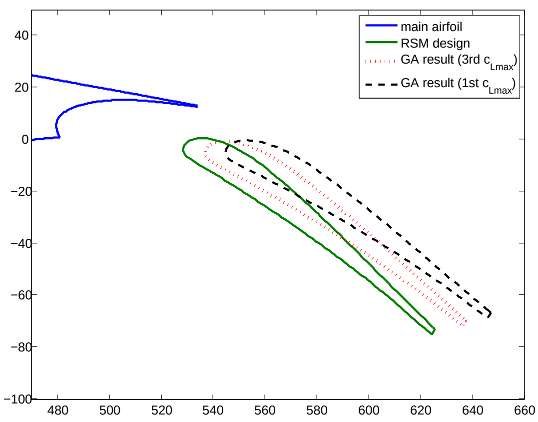

Fig. 17 Flap - optimized positions

Conclusion

It was managed to demonstrated the optimization procedure which consists of the DoE and RSM in connection with the evolution algorithm using very small population. In case of the initial vector of design parameters from RSM was used, the time needed for to find the locus of optima by μARMOGA was lower as compared with the optimization started from the baseline configuration.

The gradient vector of the RSM was not evaluated. This is probable the reason for the relatively big differences between the positions of the slat and flap from the RSM and μARMOGA. Evaluation of this gradient can be useful to find the optimal response. Experimentation along the gradient direction should continue until curvature is detected or other limitations are reached. Consequently new design matrix is created and evaluated.

The choice of the proper cost function can very affect the behavior of the lift curve. The maximization of the C_L resulted in the sharp peak of the lift curve. On the other hand the usage of the 3rd value of C_L as a cost function created the lift curve with the better behavior (the flow separation on the flap for small AoA was suppressed and the exploitable range of AoA was widened).

References

[1] Rumsey, C. L. and Ying, S. X., *Prediction of High Lift: Review of Present CFD Capability*, Progress in Aerospace Sciences, Vol. 38, No. 2, 2002, pp. 145-180

[2] Smith, A. M. O., *High-Lift Aerodynamics*, Journal of Aircraft, Vol. 12, No. 6, 1975, pp. 501-530

[3] van Dam, C. P., *The Aerodynamic Design of Multielement High-Lift System for Transport Aircraft*, Progress in Aerospace Sciences, Vol. 38, No. 2, 2002, pp. 101-144

[4] Lynn, R., *Technical report C5.2 Short-chord flaps*, HELIX/TR/QinetiQ/C5.2/RL150803/2, August 2003

[5] Tyssel, L., *Hybrid Grid Generation for Complex 3D Geometries*, Proceedings of the 7th International Conference on Numeric Grid Generation in Computational Field Simulation, Whistler, British Columbia, Canada, Sept. 2000, pp. 337-346

[6] Eliasson, P., *EDGE, a Navier-Stokes Solver for Unstructured Grids*, Proceedings to Finite Volume for Complex Applications III., ISBN 1 9039 9634 1, ISTE Ltd., London, 2002, pp 527-534

[7] Hellsten, A., *New Advanced k-ω Turbulence Model for High Lift Aerodynamics*, AIAA Journal, Vol. 43, No. 9, Sept. 2005, pp. 1857-1869

[8] Montgomery, D. C., *Design and Analysis of Experiments*, 7^{th} edition, John Wiley & Sons, Inc. 2009

[9] Schmidt, S. R., Launsby, R. G., *Understanding Industrial Designed Experiment*, 4^{th} edition, Air Academy Associates, Colorado Springs, CO, 2005

[10] Myers, R.H., Montgomery, D. C., *Response Surface Methodology*, 3rd ed., John Wiley & Sons, Inc., New York, 2009

[11] Arakawa, M., Hagiwara, I., *Development of Adaptive Real Range (ARRange) Genetic Algorithms*, JSME International Journal, Series C, Vol.41, No. 4, pp. 969-977, 1998

[12] Oyama, A., *Wing Design Using Evolutionary Algorithms*, PhD Dissertation, Department of Space Engineering, Tohoku University, March 2000

[13] Szöllös A., Šmíd, M., Hájek, J., *Aerodynamic Optimization via Multi-objective Micro-genetic Algorithm with Range Adaptation, Knowledge-Based Reinitialization, Crowding and ε-Dominance*, Advances in Engineering Software, Vol.40, No.6, June 2009

[14] Hájek, J., Szöllös, A., Šístek, J., *A new mechanism of maintaining diversity of Pareto archive in multi-objective optimization*, Advances in Engineering Software, Vol. 41, No. 6, pp. 1031-1057, 2010

Copyright Statement